6B.3 Impacts of Wind Farms on WSR-88D Radars

Donald W. Burgess
Cooperative Institute for Mesoscale Meteorological Studies, University of Oklahoma/NSSL, Norman, OK

Timothy D. Crum and Richard J. Vogt
NEXRAD Radar Operations Center

1. INTRODUCTION

The use of wind farms in the United States to generate electricity is growing dramatically (http://www.awea.org/faq/instcap.html). The amount of installed generation capacity has grown from ~2,500 mW in 2000 to greater than 12,000 mW in 2007. Wind farms now produce enough electricity to power the equivalent of 2.5 million homes. Continued growth in the number of wind farms is expected. In his 2006 Advanced Energy Initiative, President Bush stated that areas with good wind resources have the potential to supply up to 20% of the US electricity consumption. Wind farms currently produce less than 1% of the US electricity consumption today. Wind farms can have well over 100 turbines with blade tip heights over 130 m (430 ft) above ground level (AGL). Blade-tip heights of over 180 m (600 ft) AGL are expected within a few years. Blade tip velocities can approach 80 m/s, rendering the wind farms immune to normal radar clutter removal processes.

Results of research in this paper and in other recent work (Burgess *et* al 2007, Vogt *et al* 2007a and 2007b) show that when wind farms are located "close" to Weather Surveillance Radar-1988, Doppler (WSR-88D) systems, the wind farm towers and rotating blades can impact radar data quality and the performance of radar algorithms. Since data from WSR-88D radars are key components in the decision making process of issuing severe weather warnings and weather forecasts, and in supporting air traffic safety, it is important to document the known impacts. This paper addresses some of those impacts.

Policy considerations associated with wind farm placement and expansion are not addressed here, but are the subject of another paper at this conference (Vogt *et al* 2008).

2. DATA SOURCES

Wind farm impact on weather radars occurs when the towers/blades are within Radar beam Line-Of-Sight (RLOS). Even more impacts occur for towers/blades that are extremely close to the radar (<~10 km range). To document impacts and to develop a climatology of radar wind farm observations for wind farms within RLOS, the WSR-88D radar at Dodge City, KS (KDDC) was chosen for study. To document impacts for a wind farm extremely close to a radar, the WSR-88D at Great Falls, MT (KTFX) was chosen. The lead author examined lower-resolution KDDC radar product images (archive level III) for a several month period from January until May of 2007. The image data were used to construct a climatology of wind farm echo observation for the RLOS case. When interesting/hazardous weather phenomena occurred, high-resolution digital KDDC data (archive level II) were obtained and examined in detail to document impacts. A combination of low-resolution products and high-resolution digital data was used to document impacts at KTFX for a similar interval of time.

a. DODGE CITY WIND FARMS

There are two wind farms within the RLOS of the 0.5° beam of KDDC. The southwest wind farm (SW) is large (170 towers and turbines), producing a well-distributed echo centered at approximately 40 km range (Fig. 1). The northeast wind farm (NE; 72 towers and turbines) is not as large as SW, but at a center range of ~22 km it too produces a distinctive radar echo (Fig. 1). Note that the land surface rises to the west of the radar and falls to the east. Therefore, the beam height rings around the radar (colored areas in Fig. 1) are not symmetric. This allows turbine blades to be within the beam line-of-sight at longer ranges to the west. Based on nearest town locations, the SW wind farm is called the Montezuma Wind Farm, and the NE wind farm is called the Spearville Wind Farm.

b. GREAT FALLS WIND FARM

A small wind farm, 6 turbines and towers, is located very close to KTFX (Fig. 2). The centroid of the small wind farm is ~6 km from KTFX. For such near-range targets, there is no need to perform an echo climatology…echoes show up on virtually all low-elevation radar scans. However, with only 6 towers/turbines, it shows up as a very small echo.

3. CIMATOLOGY OF KDDC WIND FARM ECHOES

Typical KDDC views in clear-air mode (Fig. 3) and precipitation mode (Fig. 4) reveal the appearance and geometry of the wind farm returns. From Fig. 4, it is easy to see how wind farm returns might be mistaken for isolated showers/thunderstorms or for heavier storms within a line of echoes. Average max reflectivity at 0.5^o elevation for the larger SW wind farm is 40–50 dBZ. Average max 0.5^o values for the smaller NE wind farm are somewhat less (30-40 dBZ). Because of the large size of the SW wind farm (larger number of towers and turbine blades), partial beam blockage is seen on KDDC reflectivity images as a slight shadow down range from SW during widespread precipitation events (Fig. 5). Although radar echoes from both wind farms are seen at 0.5^o elevation angle a vast majority of the time, echoes from either wind farm grow more rare as the elevation angle increases to 0.9^o and 1.3^o (sidelobe returns during normal propagation conditions). Wind farm echo observation at and above 1.5^o elevation angle is extremely rare.

Because wind farm returns are seen most of the time, but not all of the time, when calculations show that both wind farms are within the 0.5^o beam, a quantitative climatology of wind farm echoes was constructed. Observations of both wind farms were made 8 times per day (every three hours) for the period 20 January to 20 April; a total of 91 days. The 728 observations included clear air and precipitation situations. Data loops were utilized to better understand echo evolution between observation times. The results (Fig. 6) indicate the diurnal and overall frequency of SW and NE echoes greater than 5 dBZ. Echoes >5(>20) dBZ were observed from SW 86%(77%) of the time. Echoes >5(>20) dBZ were observed from NW 97%(81%) of the time. The wind farm further from the radar (SW) exhibited a diurnal trend, being observed more frequently in the early morning and less frequently in the late afternoon. The wind farm closer to the radar (NE) did not display a noticeable diurnal trend.

More attention was given to those observation times when no echoes from the wind farms were observed. Additional study of hourly DDC surface observations and 12-hourly DDC soundings revealed that all times of no echo resulted from two sources: 1) sub-refraction-type beam propagation (beam heights higher than normal propagation), and 2) near calm wind speeds. A sub-refraction example (Fig. 7) shows the loss of echo from SW after 19Z, not returning until 03Z. The 00Z sounding features a low-level dry adiabatic lapse rate. Hourly surface observations indicate late afternoon warming and after dark cooling. At no time did observed surface wind speeds fall to near-calm conditions. A near-calm wind speed example (Fig. 8) shows the loss of echo during the night when DDC wind speeds became calm. A nearby sounding (LMN, Lamont, OK; DDC was unavailable) and DDC surface temperatures suggest that substantial inversions/lapse rates didn't occur during the night. It is assumed that when the blades don't turn during light wind conditions, radar ground-clutter-suppression processing successfully removes the returns from the towers and stationary blades.

4. IMPACTS OF KDDC WIND FARMS

The most common impact of the wind farms is judged to be false storm identification. Examples in Fig. 9 indicate the possibility that wind farm echoes could easily be mistaken for stronger storms/maximum precipitation areas within echo lines and echo areas. Wind farm return also might be mistaken for a newly-developing storm at the edge of a storm area (Fig. 9-left). A second common impact of the wind farms is the production of velocity dealiasing algorithm errors produced by the wind farm area of disturbed/contaminated velocities (Fig. 10). Wind-farm-associated velocity dealiasing errors occur in both clear-air and precipitation situations. Both error sources contaminate input data and cause errors in other algorithms. An example of a Mesocyclone Detection Algorithm false alarm is shown in Fig. 11. With the radar in Volume Coverage Pattern 12, disturbed velocity returns from 0.5^o and 0.9^o were sufficient to satisfy horizontal shear and vertical continuity requirements for mesocyclone detection even though no real storm or mesocyclone was present. Of course, during precipitation situations, input wind farm echoes will always produce false precipitation accumulation estimates. WSR-88D Precipitation Processing System software allows for the creation of exclusion zones where known areas of contaminated data are removed from accumulation estimation. This technique partially mitigates the erroneous accumulation estimates but produces regions of no estimate and loss of output continuity (Fig. 12). Note that at the time of this study, DDC personnel had created an exclusion zone for the first-built SW wind farm, but had not done so for the later-built NE wind farm. Such condition allows for observations with and without exclusion zones. False precipitation accumulation estimates for NE are as high as 13 inches for a thunderstorm event, and as high as 12.7 inches for a continuous light rain event. Also note the precipitation accumulation "shadow" produced by

SW-generated attenuation, particularly noticeable in Fig 12 (upper right).

It should be mentioned that at no time during the study period was there a product (warning, short-range forecast or current weather statement) from the DDC WFO that was found to be in error because of non-precipitation wind farm radar return or false algorithm output. Discussion with staff at the DDC WFO indicated that they had become familiar with the wind farm echoes and mentally removed them from consideration during product preparation. Of course, the potential for a product error always exists, particularly during stressful warning operations. It also should be mentioned that other radar data users (beyond the local WFO) might not be as familiar with the wind farm returns, resulting in susceptibility to errors in data analysis and product generation. In particular, users of radar data mosaics and algorithm outputs (in general those not frequently examining the base data) would be more susceptible to error problems. Of course, automated systems, such as used by the FFA and others, would be very susceptible to output errors caused by wind farm returns.

5. IMPACTS OF THE KTFX WIND FARM

The biggest concern with the small wind farm very close to KTFX is the multipath beam scattering and return which produces a region of disturbed velocities many kilometers beyond the location of the wind farm (Fig. 13). Because of the very close range of the wind farm, disturbed velocities show up on several lower elevation angles. The extended region of disturbed velocity shows up in clear air and light-to-moderate precipitation situations, being superseded only in heavy precipitation with strong radar returns. The disturbed velocity region also produces a significant number of velocity dealiasing errors.

These characteristics are manifested in significant impacts to velocity interpretation in the extensive disturbed velocity region. In particular, detection and tracking of clear-air wind boundaries near and northwest of KTFX was noticeably reduced. An important impact was noted to one algorithm, the VAD Algorithm and its associated VAD Wind Profile (VWP). Since the region of disturbed velocity is large, a significant sector of the VAD circle is affected and erroneous VWP estimates are produced. The example in Fig. 14 shows the type of errors that occur. The 2 March case was a light snow event with a wide and extended-range disturbed velocity region that persisted for several hours. The region of disturbed velocities had serious impact on the VWP output, producing long-lasting and large vertical height interval of erroneous wind estimates that in no way resembled the vertical wind profile from the TFX sounding. VWP inputs are assimilated into NWS numerical models and used in automated fashion as inputs to other models and forecast systems. Extensive erroneous VWP data, as with the 2 March case, could produce flawed model output and inaccuracies in both human and automated forecast products.

6. SUMMARY

Based on extensive data analysis of two wind farms within Radar-Line-Of-Sight (RLOS) of the KDDC WSR-88D and one farm at very close range to the KTFX WSR-88D, estimates can be made of potential impacts to all radars within the NEXRAD Network.

a. RLOS BASE DATA IMPACTS

All wind farms within RLOS of WSR-88D radars have at least some potential impacts to base data and to algorithms.

1. False echoes appear in reflectivity data because ground-clutter cancellation techniques fail to identify the echoes as ground clutter. Partial beam blockage occurs with small reduction in reflectivity estimates.
2. Disturbed areas are introduced into radial velocity data...noise-like mean velocity estimates. Velocity dealiasing errors occur frequently and spread to areas beyond the wind farms.
3. Erroneous velocity spectrum width values (approximating velocity components spread across the entire Nyquist co-interval) are introduced.

b. RLOS ALGORITHM IMPACTS

4. Erroneous PPS Algorithm precipitation estimates (extremely high values) occur unless exclusion zones are invoked. If exclusion zones are invoked, some loss of data occurs.
5. Mesocyclone Detection and Tornado Detection Algorithm errors occur in the form of false alarms with potential for missed detections.
6. Errors will occur with the soon-to-be-installed Turbulence Detection Algorithm in the form of false alarms.

c. EXTREMELY CLOSE RANGE IMPACTS

Wind farms at extremely close ranges to radars have all the impacts listed above plus additional ones.

7. Inter-turbine scatter and multi-trip/multi-path

echoes expand wind-farm-related radar returns (radial velocity, spectrum width, and to some extent, reflectivity) to extended ranges and wide azimuth sectors. Relatively large regions of affected data are produced.

8. VWP Algorithm errors occur in the form of inaccurate environmental wind estimates that in turn affect numerical model assimilations and forecasts.

9. The disturbed velocity regions are likely to cause errors/missed detections by the Machine Intelligent Gust Front Algorithm (MIGFA).

10. Large wind farms at very close range to radars (a geometry not yet studied) could potentially produce extremely large areas of beam blockage, resulting in significant loss of data and large radar network loss of coverage.

d. CURRENT LIMITATIONS OF RESULTS

To date, only data from a few wind farms that are within RLOS of radars or, worse, at very close range to radars have been analyzed. It is possible that additional impacts, not yet seen, will occur at other radar sites. Any conclusions regarding wind farm impacts on WSR-88D radars should be considered preliminary until more data from additional radars are analyzed. In particular, large wind farms with tall turbine tops at very close ranges to radars, a worst case scenario, could have even more scattering phenomenon and attention affects than have as yet been detected or estimated. Further study of wind farm impacts to WSR-88D radars is warranted.

7. ACKNOWLEDGMENTS

Funding was provided by NOAA/Office of Oceanic and Atmospheric Research under NOAA-University of Oklahoma Cooperative Agreement #NA17RJ1227, U.S. Department of Commerce. Funding was provided by the NOAA NEXRAD Radar Operations Center. Thanks are given to Kevin Manross, CIMMS/NSSL, for assistance with WDSSII data analysis. Thanks are given to Radar Operations Center/Applications Branch personnel (Dave Zittel, Bob Lee, and Melissa Pitchin) for ORPG product and algorithm replay assistance. Thanks to Ron Guenther (RS Information Systems, Inc; ROC Support Contractor) for mapping/graphics support.

7. REFERENCES

Burgess, D.W., T. Crum, and R.J. Vogt, 2007: Impacts of wind turbine farms on WSR-88D radars. *33rd Int. Conf. on Radar Meteorolog*, Cairns, Australia, Amer. Meteor. Soc., Paper, 13B.6.

Vogt, R.J., J.R. Reed, T. Crum, J.T. Snow, R. Palmer, B. Isom, and D.W. Burgess, 2007a: Impacts of wind farms on WSR-88D operations and policy considerations. Preprints, *24th Int. Conf. on Interactive Information Processing Systems (IIPS) for Meteorology, Oceanography, and Hydrology,* San Antonio, TX, Amer. Meteor. Soc., Paper 5B.7.

_____ , T. Crum, J.R. Reed, C.A. Ray, J. Chrisman, R. Palmer, B. Isom, D. Burgess, and M. Paese, 2007b: Weather radars and wind farms – working together for mutual benefit. Preprints WINDPOWER 2007, *American Wind Endergy Association Conference and Exhibition*, Los Angeles, CA.

_____ , _____ , J.T. Snow, R.D. Palmer, B. Isom, and D. Burgess, 2008: An update on policy considerations of wind farm impacts on WSR-88D systems. *24th Int. Conf. on Interactive Information Processing Systems (IIPS) for Meteorology, Oceanography, and Hydrology,* New Orleans, LA, Amer. Meteor. Soc., Paper 6B4.

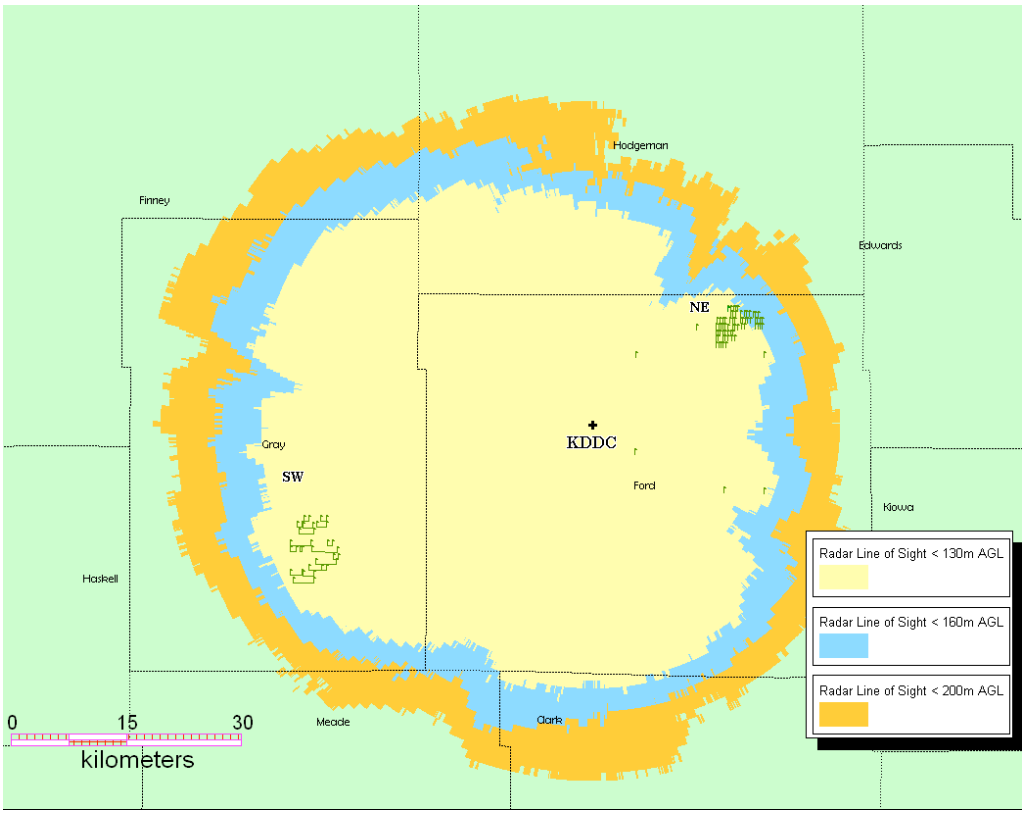

Figure 1. Location of southwest (SW) and northeast (NE) wind farms and KDDC WSR-88D. Shading indicates 0.5^{o} elevation beam coverage at specified heights AGL.

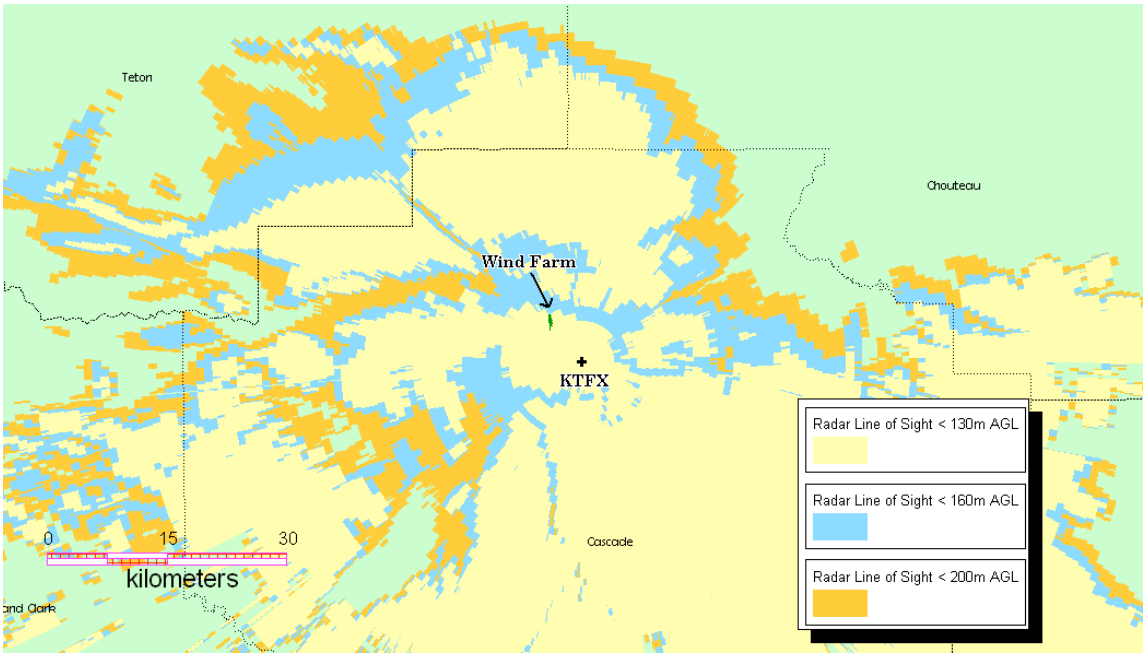

Figure 2. Same as Fig. 1 except location of wind farm and KTFX WSR-88D.

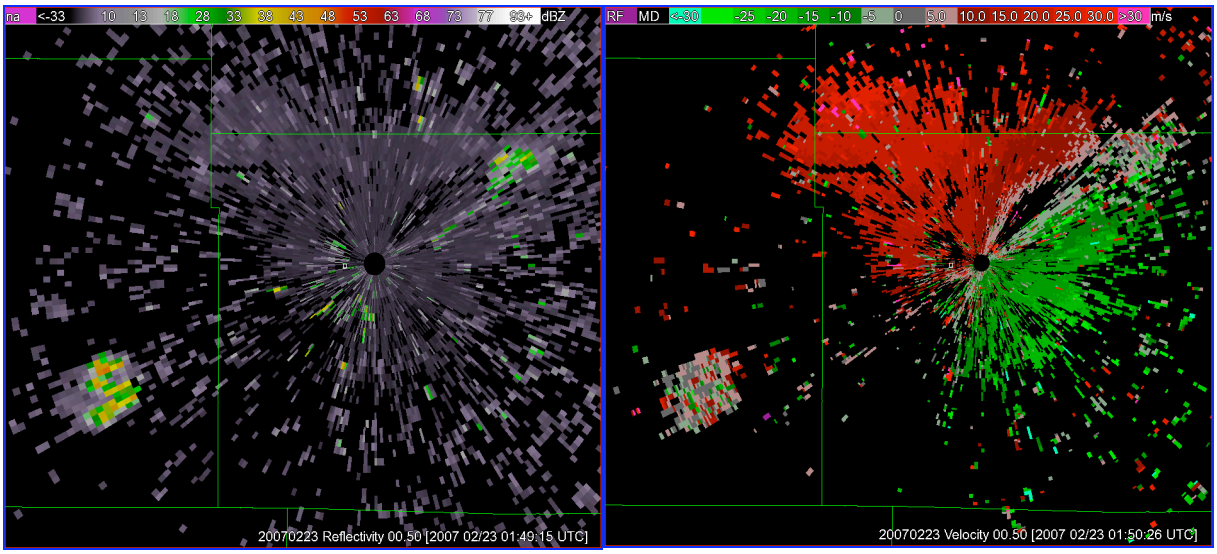

Figure 3. Typical KDDC clear-air-mode depiction of the SW and NE wind farms, reflectivity (left) and velocity (right).

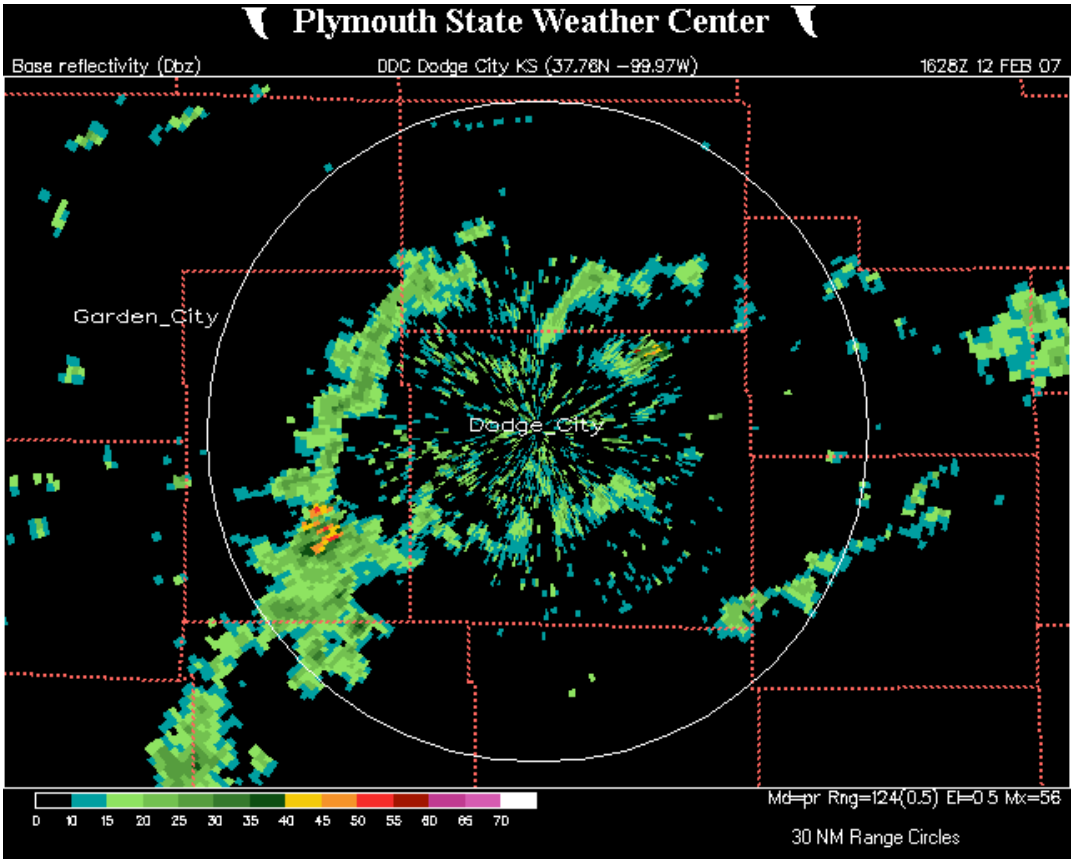

Figure 4. Typical KDDC precipitation mode depiction (reflectivity) of the SW and NE wind farms

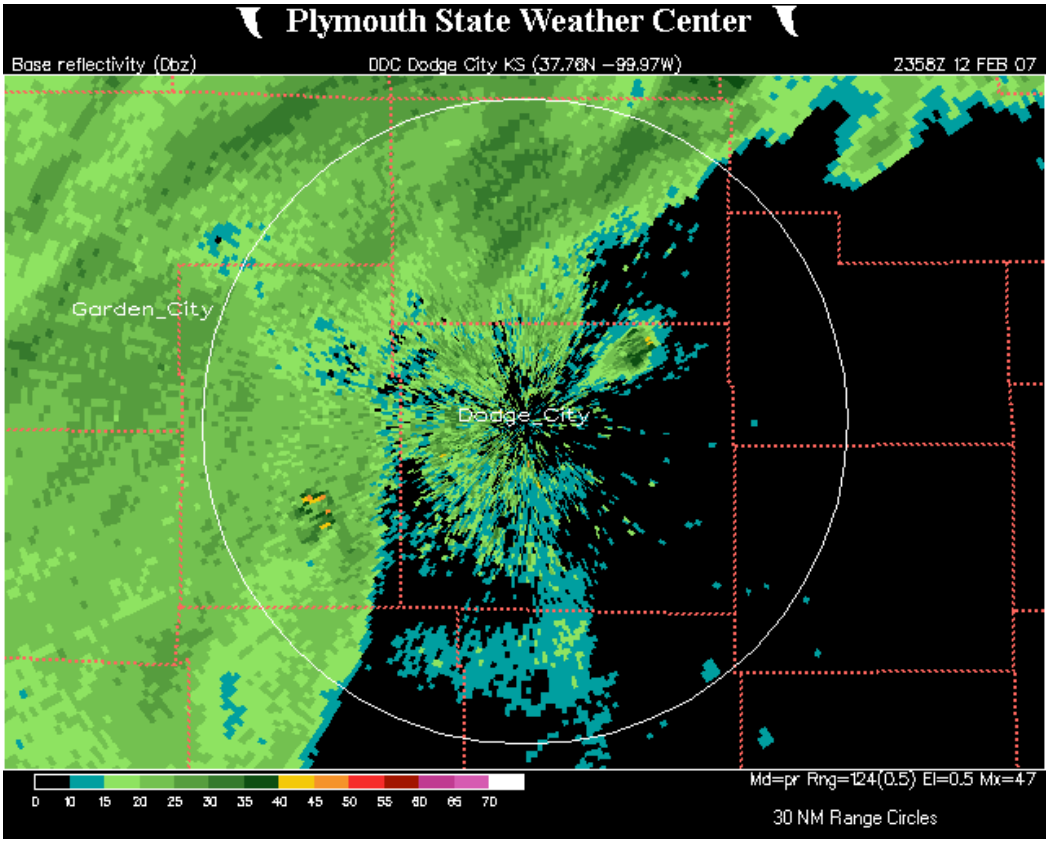

Figure 5. KDDC reflectivity display during a widespread precipitation event. Note the partial beam blockage to the southwest of the SW wind farm.

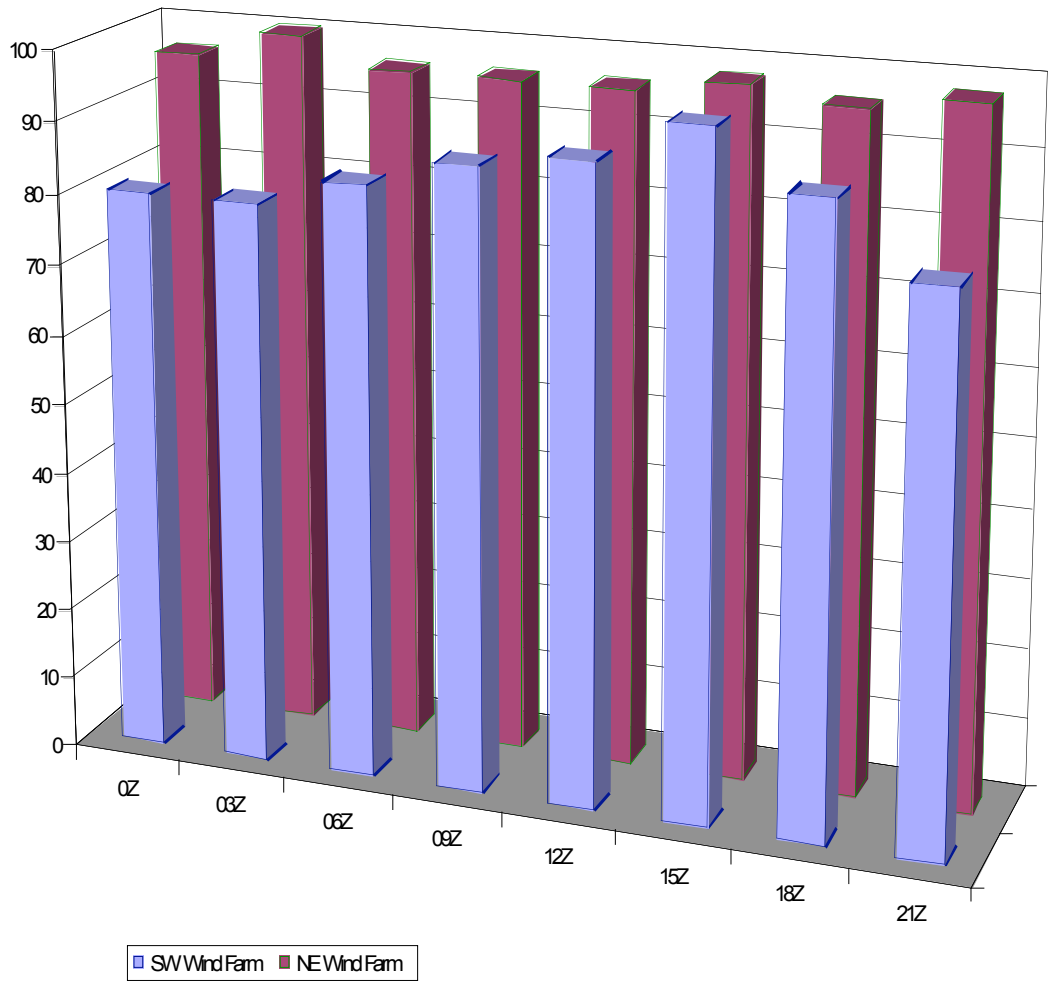

Figure 6. Climatology of radar echoes >5 dBZ for SW and NE wind farms. Ordinate is percentage of observation. Abscissa is time (UTC) of observation.

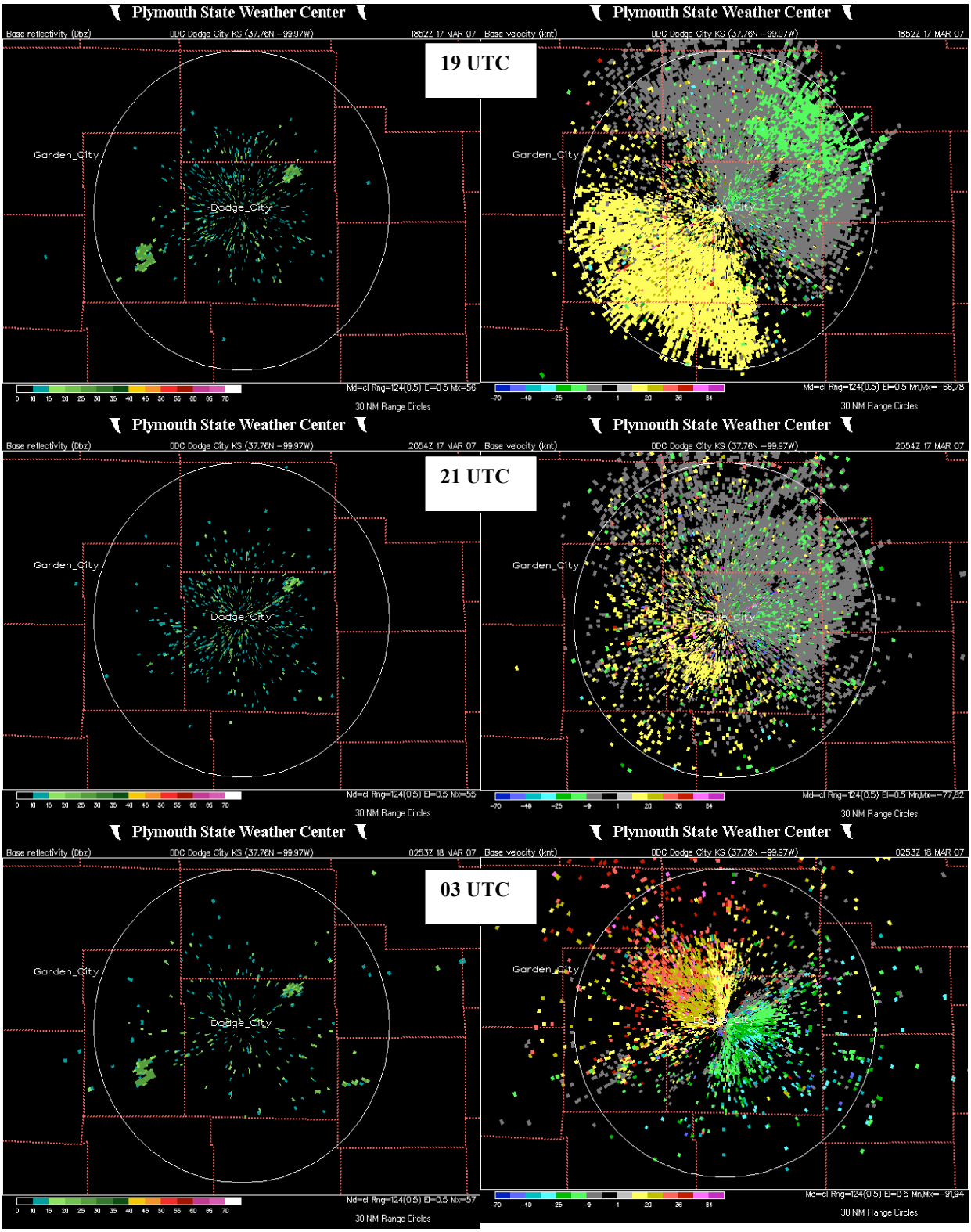

Figure 7. KDDC 0.5° reflectivity and velocity at three times, continued.

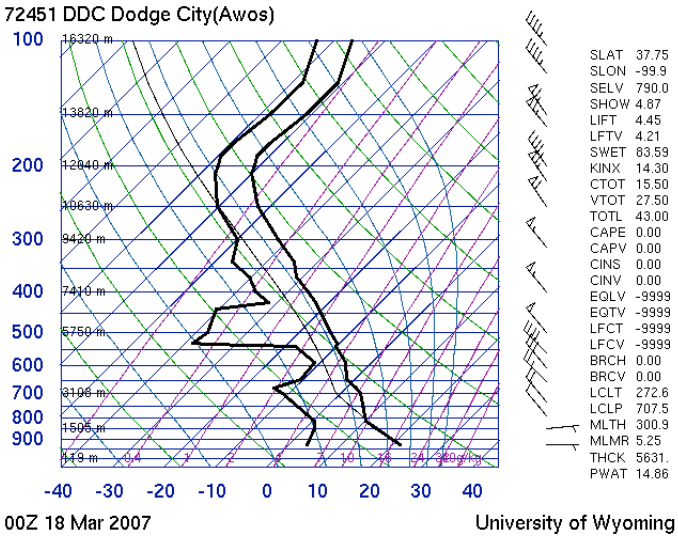

DDC Surface Observations

Time(UTC)/T(F)/DpT(F)/Wnd Dir@Speed (kt)

19Z 68/38/03@13
21Z 73/39/06@08
00Z 67/42/08@10
03Z 60/40/16@10

Figure 7, Continued. DDC upper air sounding and surface observations for 17 March 2007. Loss and reappearance of SW wind farm echo thought to have occurred because of development/ending of sub-refraction conditions.

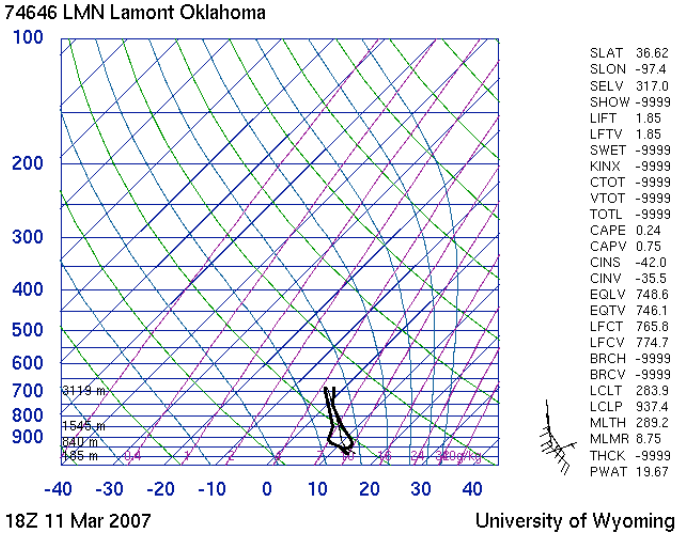

DDC Surface Observations

Time/CurrentWeather/T(F)/dpT(F)/Wnd Dir@Speed(kt)

00Z Fog/49/47/35@07
06Z Fog/48/47/CALM
12Z Fog/46/44/30@09

Figure 8. Lamont, OK upper air sounding and DDC surface observations for 10 and 11 March 2007.

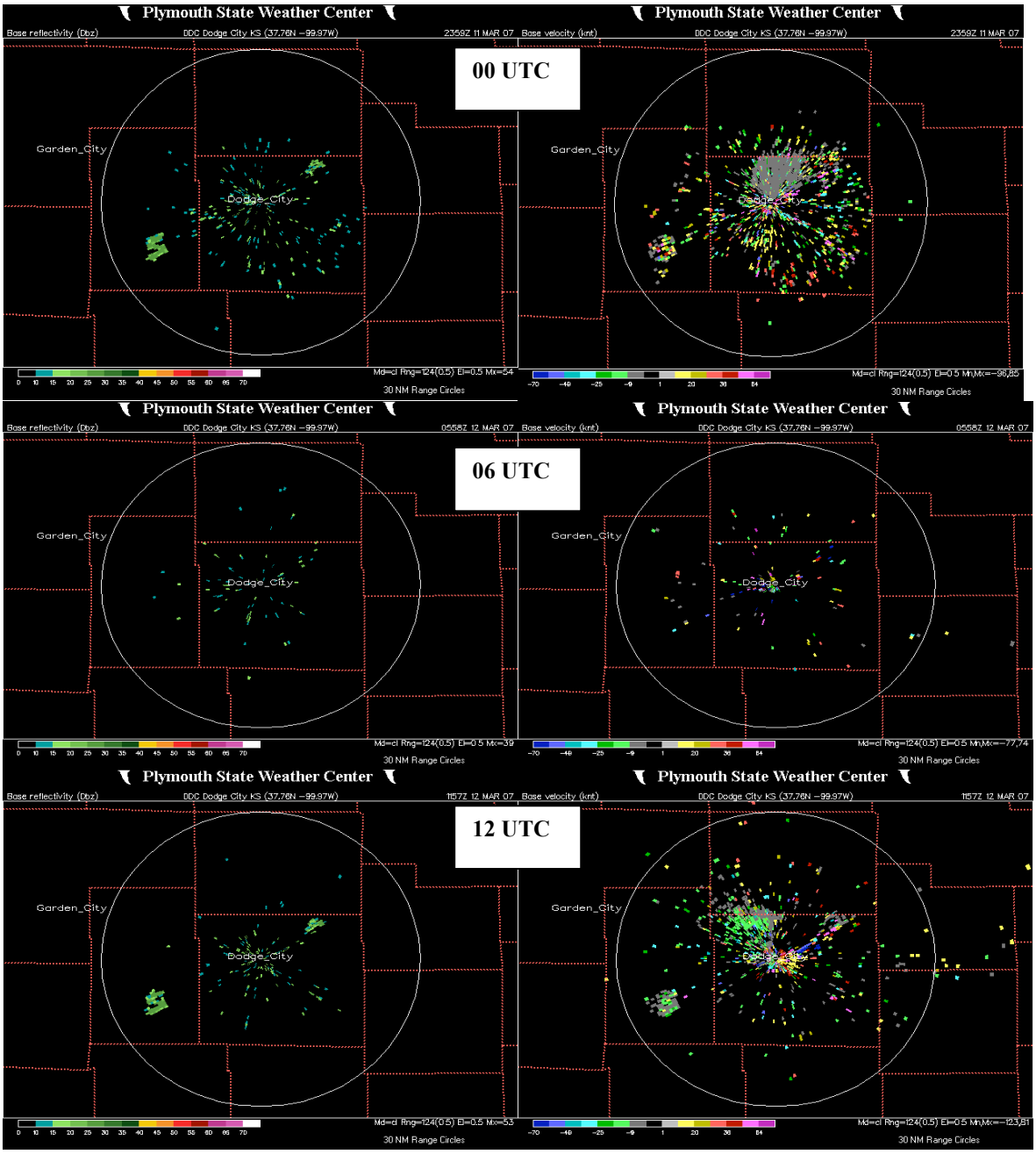

Figure 8, Continued. KDDC 0.5° reflectivity and velocity at three times for 10 and 11 March 2007. Loss and return of SW and NE wind farm echo believed to occur because of onset/end of near calm winds.

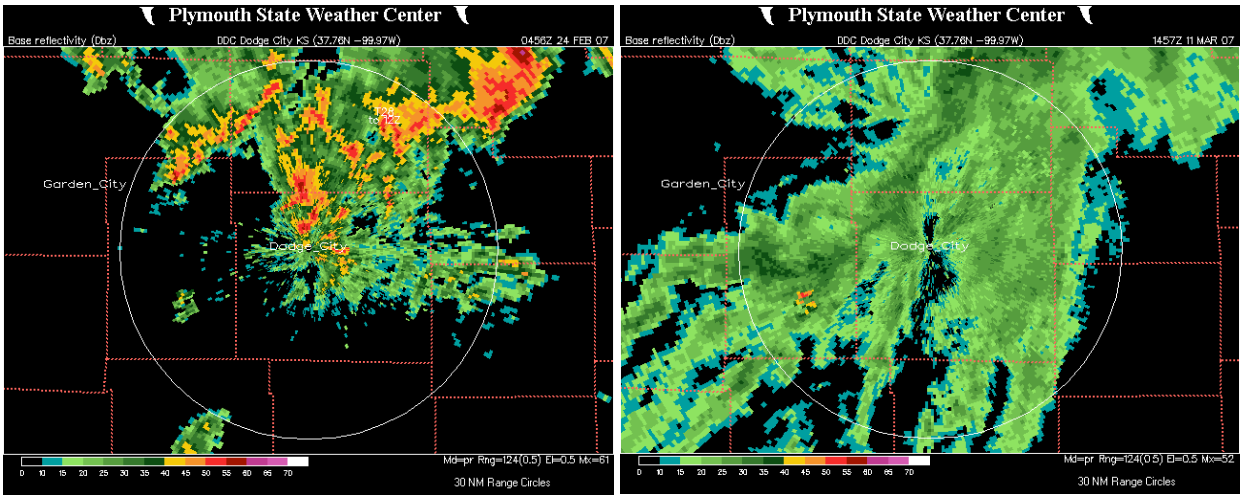

Figure 9. KDDC reflectivity images where SW wind farm could be confused with new cell development (left) and confused with a stronger cell within a line (right).

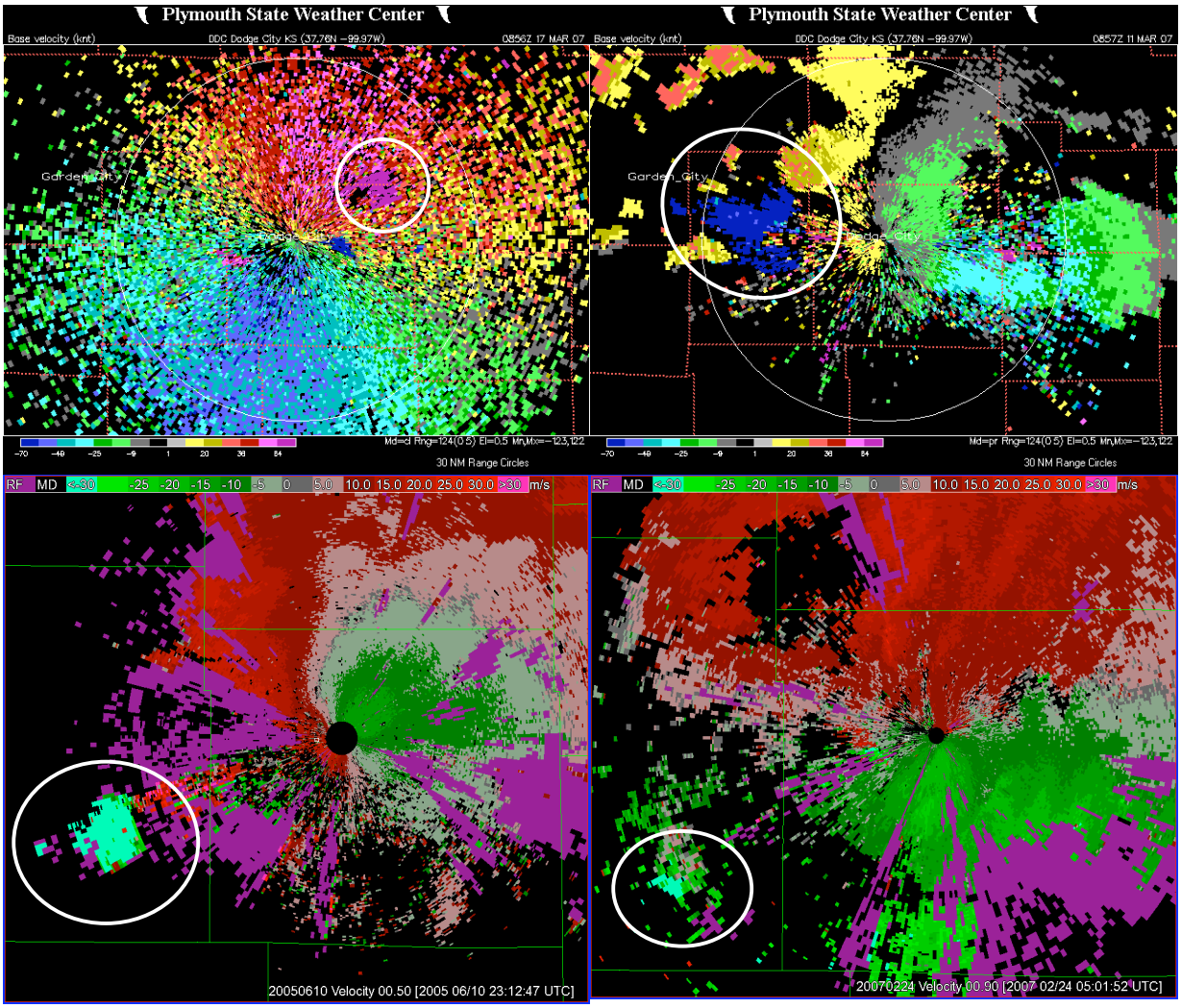

Figure 10. KDDC examples of improperly dealiased velocities caused by disturbed regions of wind farm echo. All images are 0.5^{o} elevation angle except lower right which is 0.9^{o} elevation angle.

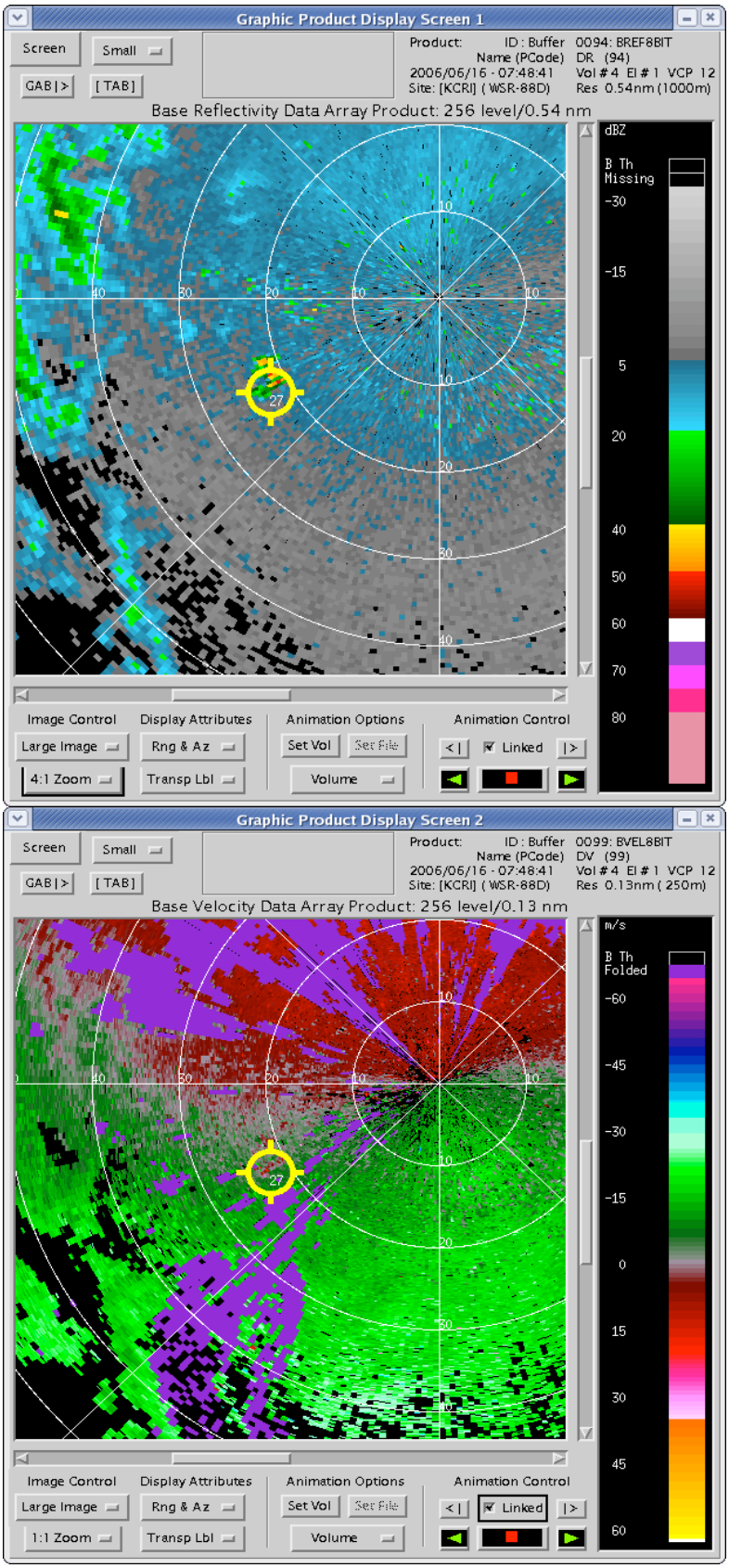

Figure 11. KDDC 0.5° reflectivity (top) and velocity (bottom) at time of false mesocyclone detection (yellow circle).

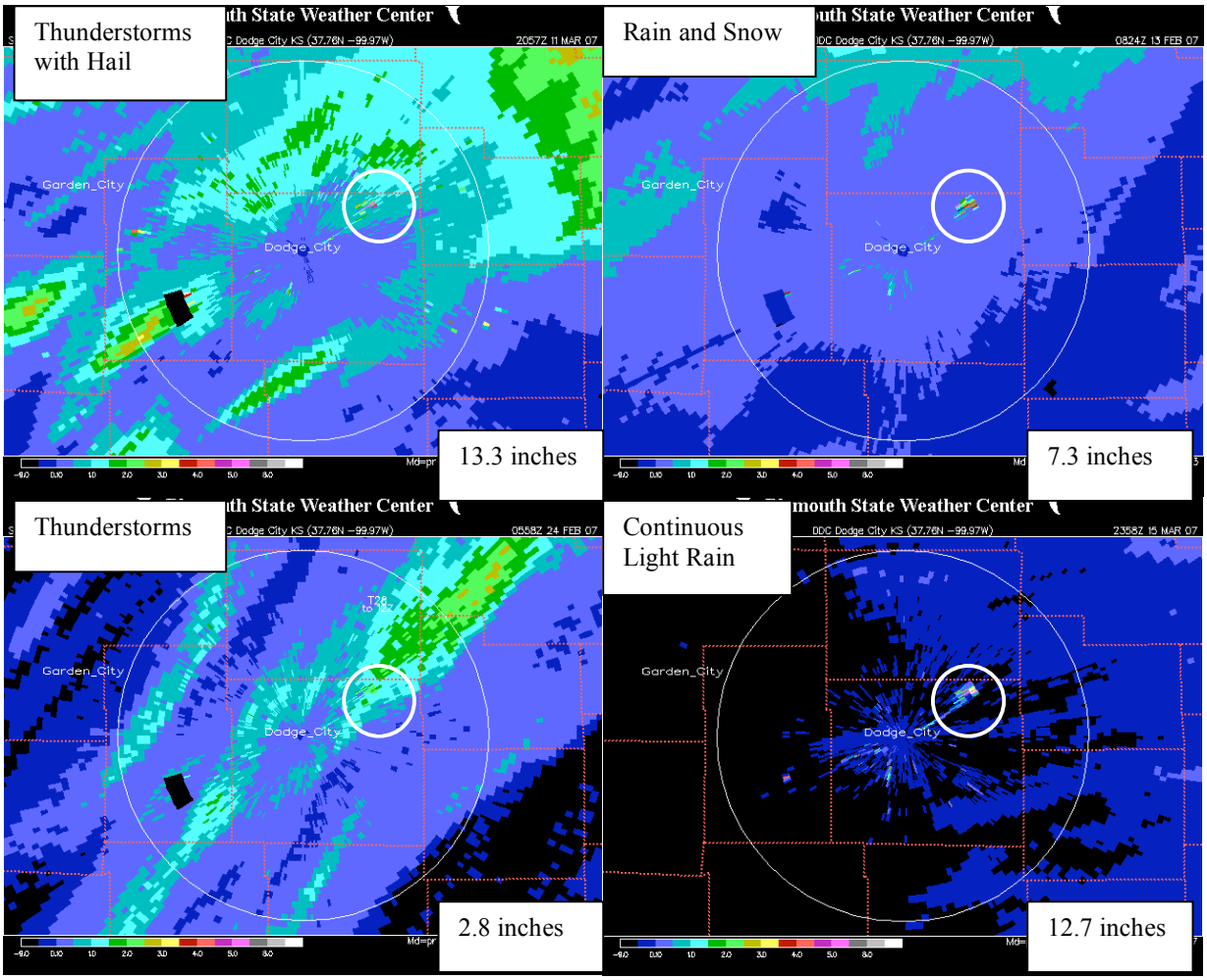

Figure 12. Four examples of wind-farm-related false precipitation estimates (Storm Total Precipitin Product) for NE wind farm (circled), max accumulation shown in lower right. Artifacts associated with SW wind farm (partial-attenuation-produced reduced estimates down radial, and loss of continuity in exclusion zone) can be seen in all but lower right example. Precipitation event type shown for each example (upper left).

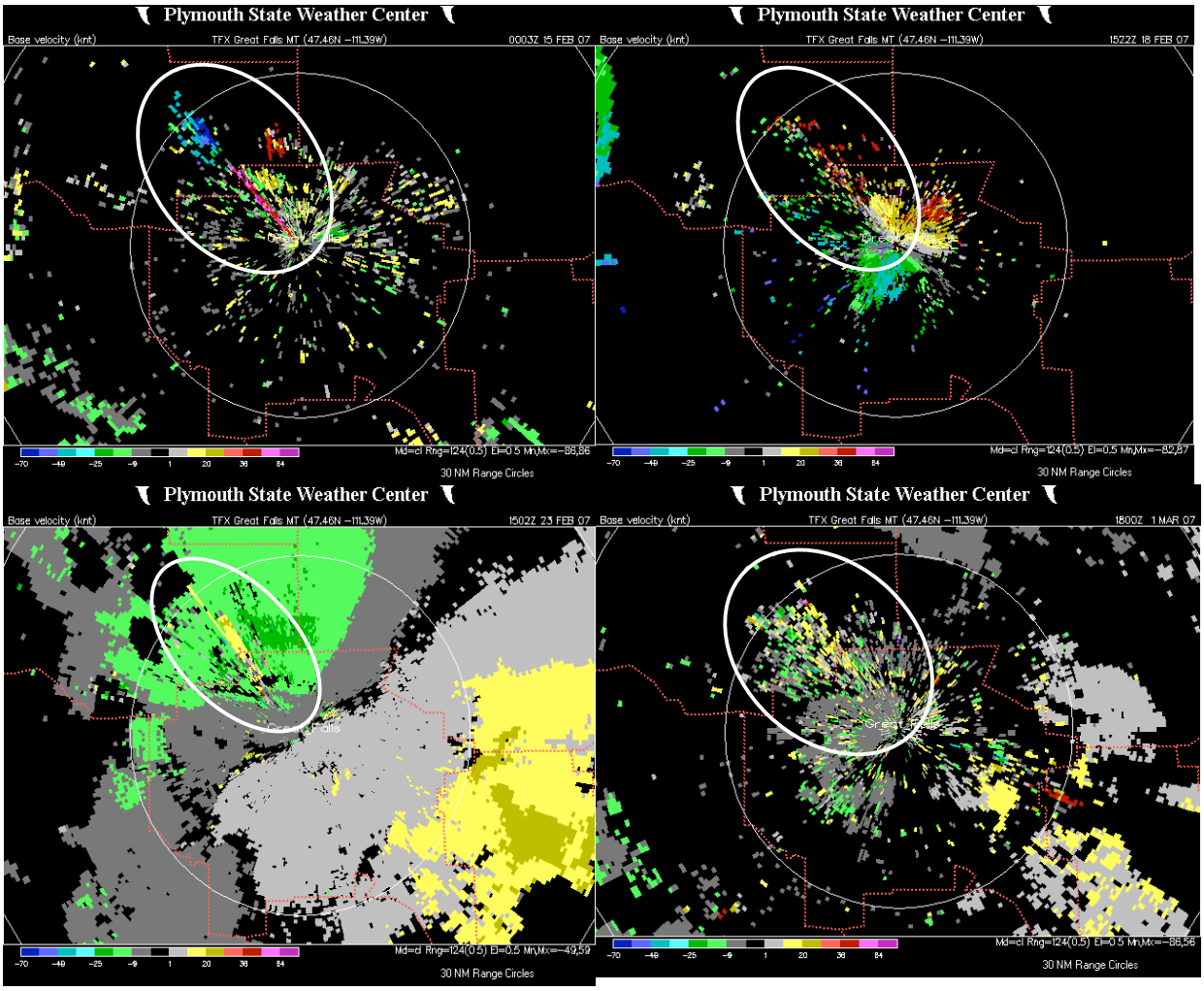

Figure 13. Four examples of KTFX disturbed velocities (enclosed white ovals) caused by very-close-to-the-radar wind farm. Top two examples are clear-air mode, and bottom two examples are precipitation mode. Extent of disturbed velocity area can be visualized by noting that radar range circle is at 56 km (30 nm).

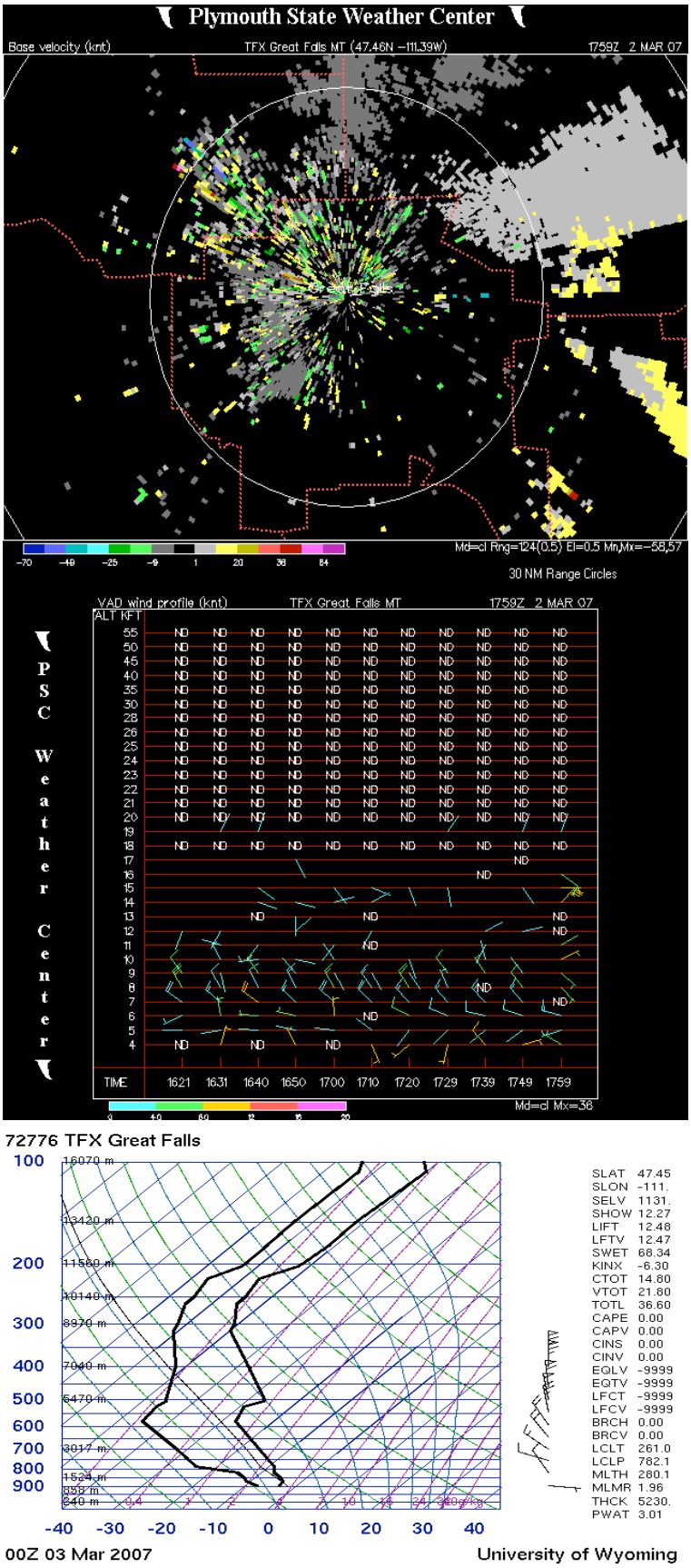

Figure 14. KTFX example of extended period of disturbed velocity (one time in upper panel), erroneous VAD Wind Profile (VWP) Algorithm output contamined by erroneous input velocity data (middle panel), and TFX sounding showing true upper wind profile. Note large difference between direction and speed of wind barbs shown in middle and lower panels.